Contents

1 Discussion

Contents

The treatment planning results presented in the previous chapters are the first feasibility study to investigate the use of carbon ions for a non-invasive treatment of atrial fibrillation (AF). Currently existing treatment procedures for this cardiac arrhythmia have major drawbacks and due to the prevalence of this condition a new treatment modality would be beneficial [**?**] [**?**]. It could be shown that scanned ion beams have the potential to become an accurate, fast and non-invasive treatment approach for AF.

Cardiac target volumes like the pulmonary veins (PVs) or the atrioventricular (AV) node move due to respiration of the patient as well as due to heartbeat. When treating moving targets with a scanned carbon ion beam interference effects between the particle delivery and the inter-fractional target motion are observed, leading to over and under dosages in the target volume and hence endangering the treatment outcome. Motion mitigation techniques are thus needed, which were studied independently for the respiratory and heartbeat motion influence. Cardiac target volumes are surrounded by critical structures and organs at risk (OAR) like esophagus, trachea and aorta. A detailed analysis of the OAR dose depostion was carried out, which will be discussed in section 1.1.2. In section 1.1.3 special emphasis will be given to the reduced OAR dose deposition with scanned carbon ions compared to a non-invasive treatment with photons. The target volume displacement will be discussed in section 1.2.1. Afterwards the findings of treatment planning studies with motion mitigation techniques will be discussed in section 1.2.3.

1.1 Dose deposition

In the here presented feasibility study of a non-invasive treatment of AF with carbon ions, a physical dose of 25Gy was applied in all treatment plans. This dose was chosen according to the publication by Sharma et al. [Sha10] in which it was stated as the minimal needed dose in order to see an electrophysiological effect induced by photon irradiation. Older studies with photon irradiations in animal models support the finding by Sharma et al. in which doses higher than 20Gy seem to be sufficient in order to induce fibrotic tissue [Faj70] [Faj73]. A short overview will be given in section 1.1.1.

A close analysis of the dose deposition to the OARs was carried out in the here presented work. Human data was studied for PVs ablation (chapters **??** and **??**). In preparation for animal studies, which will be carried out at GSI in 2014, the irradiation of the AV node in pigs was analyzed (chapter **??**). The findings will be discussed in section 1.1.2 and a comparison with photon irradiation will be given in 1.1.3. For critical structures like the aorta, esophagus, trachea and the heart itself dose-volume limits from SBRT were used [RTOG0631] [RTOG0915]. As the heart is not only an OAR in this studied treatment, but the target site itself, the dose-volume limits for this organ were often exceeded. Closer analysis of the irradiated cardiac substructures was hence performed.

1.1.1 Dose to target area

Sharma et al. stated that a dose of at least 25Gy is needed in order to induce a change in the conduction system of the heart with photon beams [Sha10]. Nevertheless also higher doses have been applied in the animal model study, reaching up to 80Gy. Part of the planned animal experiments at GSI will be a dose escalation study, in which the needed carbon ion dose for the generation of the desired fibrosis in the target area will be examined more closely. It is already known from former studies on the effect of radiation on the heart which dose depositions as single fraction doses are sufficient in order to induce fibrotic tissue [Faj70] [Faj73] [Phi64] [Bis65] [Ste68] [Efs56].

Fajardo et al. [Faj70] [Faj73] investigated the evolution of radiation induced myocardial damage after a single dose of 20Gy in rabbits as well as a fractionated treatment, both with 6MV photons. They stated that their findings were independent of the time course of the irradiation, hence if the dose was applied as a single fraction or in different fractions. They found that there are three distinct stages in the evolution of radiation induced cardiac damage and divided it into an acute phase (an inflammtion within the first 48hours), a latent stage (which can last up to seventy days) and the late stage where fibrotic lesions occur. Their explanation

for the formation of fibrotic tissue is a failure of microcirculation, resulting from a failure of the complete reconstruction of capillaries in the endothelial cells after irradiation. They state that the occuring ischemia leads to myocardium fibrosis, which becomes maximal beyond 120 days. Other studies by Phillips et al. [Phi64] and Bishop et al. [Bis65] irradiated hearts of dogs and rodents with single photon doses of 60Gy to 96Gy. Both authors stated that they found severe functional abnormalities as well as myocardial fibrosis or even necrosis [Ste68]. Efskind et al. [Efs56] found fatal myocardial damage after 80Gy photon irradiation to the heart of rabbits.

It can thus be assumed that the required dose for the desired generation of fibrotic tissue in the cardiac target volumes will require at least 20Gy, while high single fraction doses of up to 60Gy might induce necrosis, which needs to be avoided. Preliminary studies using the LEM for the calculation of biological doses in single fraction deliveries with the stated 25Gy resulted to have a RBE of 1.1. As the RBE is expected to be smaller for even higher doses, the physical dose can be considered proportional to the biological dose. Hence the dose to the target volume, as well as the dose to the critical structures, could be directly scaled to the desired value.

1.1.2 Dose to OAR

In the studied human data it was found that the dose deposition in the aorta and trachea were uncritical and did not exceed the stated dose-volume limits. This was valid for all the studied safety margins (3mm, 5mm and 7mm) of the target volume, independent of the fact that the OAR dose deposition correlates with margin size. The esophagus on the other hand is an endangered organ due to its proximity to the studied irradiation site of the PVs. Different beam directions and field channel numbers were studied in IMRT setting, none of which resulted in a satisfactory sparing of this structure. Dose-volume exceeding results were already obtained for a small safety margin of 3mm in some patient cases, or even without the usage of any margin in other cases. An IMPT(OAR) treatment was hence necessary, where the maximal dose to the esophagus was implemented in the dose optimization process. Two different IMPT(OAR) settings were used. One which was planned to deposit not more than a maximal dose of 17.5Gy (70% of 25Gy) in this organ and one with a maximal dose of 7.5Gy (30% of 25Gy) to the structure. While the weaker restriction already led to an improved result, the dose depositions were still too high, for one patient case even with only 3mm margin. The stronger restriction on the other hand resulted in dose depositions that did not exceed the dose-volume limit in all studied patient cases and for all studied safety margins. The dose restrictions for the esophagus even led to a further reduced dose deposition in the trachea of the studied patients due to the direct proximity of these two organs with respect to the used beam channel directions.

In order to guarantee a safe delivery in a potential patient application a dedicated protocol

to ensure adequate esophagus sparing is nevertheless needed. Possible solutions to detect range uncertainties before the delivery of the high single fraction dose are pre-irradiations with small doses in the order of mGy [Ben12] and the usage of in-beam PET monitoring with a probing beam [Fie10] [Lin12], which are presented in more detail in section 1.2.2. Analog to studies by Rucinski et al. [Ruc13], Christodouleas et al. [Chr13] and van Gysen et al. [Gys14] for prostate cancer or studies by Viswanathan et al. [Vis13] for gynecologic cancers it was furthermore considered if the injection of a spacer like hydrogel would be beneficial in order to increase the distance between the esophagus and the ablation sites. Due to an increased risk for infections in the cervical region this approach is considered unfeasible in this case (Prof. Christoph Bert, personal communication, April 10, 2014).

Even though the dose-volume limits for the heart were exceeded, it should be noted that the heart is also the target volume in this feasibility studied. Further analysis of the maximal point dose, the maximal irradiated volume as well as the median dose were in good agreement to limitations stated in literature [Gag10] [Mar98] [Wei08] [Han93] and hence no pericarditis should be expected. Concerning the irradiated cardiac substructures it was found that three beam directions yielded a lower mean dose to the LCA. A mean dose over all patient cases of up to 1.5Gy for 7mm safety margin was found. According to a study by Darby et al. [Dar13] major coronary events increase by 7.4% per Gy photon irradiation after five years post radiotherapy. Due to the advanced age of the atrial fibrillation patient cohort the irradiation of the coronary arteries might hence play a less significant role. Moreover, recent studies indicate that an irradiation of the heart with carbon ions might even lead to beneficial effects in the intercellular communciation. Studies by Amino et al. indicate that single fraction carbon ion irradiations of more than 10Gy lead to an increased expression of Connexin 43 (Cx43) [Ami06] [Ami10]. This protein is involved in the construction of gap junctions in mammalian hearts, which are intercellular channels enabling current flow and hence the propagation of action potentials (see chapter **??**, section **??**). It has been shown that remodelling of connexin expression and gap junction organization are featured in pathological conditions of the heart, including ischemia and heart failure [Sev04] [Sev08]. Recent studies indicate that connexin expression is also implied in the induction and sustaining of AF [Kan04] [Pol01] [Yeh01] [Bik11]. Amino et al. could show in animal models that a cardiac irradiation with carbon ions led to a dose-dependent upregulation of Cx43 expression [Ami06], lasting for at least one year [Ami10]. It was found that this result improved the conductivity and repolarization of the animal hearts, hence having the potential for an addiational antiarrhthmic effect. The clinical relevance of these findings nneds to be investigated.

Due to the anatomical differences of pigs compared to humans and due to the larger distance of the AV node to critical structures (esophagus, trachea and aorta) dose depositions

to OAR for the irradiation of the AV node in the planned animal model were found to be negligible. Dose-volume limits were not exceeded and the stated OARs as well as the radiosensitive cardiac substructures were well spared. The dose-volume limits for the heart were also not exceeded. Maximal point dose to the heart as well as maximal irradiated volume and mean dose were also in very good agreement to the literature findings for human data. Late effects due to e.g. coronary events would also not be expected from the obtained dose deposition in these structures. It should be noted that a potential detection of these events would not be feasible due to the short lifespan of the animals used in the planned animal model feasibility study planned at GSI.

1.1.3 Dose to OAR: Comparison to photons

A non-invasive treatment with carbon ions is expected to result in a better sparing of the surrounding tissue and OARs compared to an irradiation with photons. In order to study this assumption results of treatment planning studies based on the same patient data sets and the resultant dose deposition to the OAR were studied. This was carried out both for human data sets as well as porcine data sets. The photon treatment plans are courtesy of Dr. Limin Song and Dr. Amanda Deisher, Mayo Clinic, USA.

Human data

Photon treatment plans were carried out on the reference CT phase of patient 2 and patient 4 (see chapter **??**) with a 6MV photon beam. These two data sets were chosen as the carbon ion treatment plans resulted in the highest studied dose deposition to the esophagus in patient 2, while patient 4 resulted in the lowest dose deposition to this structure in the studied patient cohort. The photon plans were carried out as a seven field IMRT(OAR) treatment (see figure 1.1). The delivery was also planned as a single fraction irradiation of 25Gy. For the ITV generation the PVs target volumes were isotropically expended by 3mm. The final PTV was generated by applying an additional isotropic expension of 5mm margin to the ITV. For the carbon ion treatment, which were carried out as IMPT plans, an isoptropic safety margin of 5mm was added to the CTV. Afterwards additional ITV margins were generated from the 4DCTs, accounting also for range variations [**?**]. The IMPT plans were computed with three beam channel directions (see chapter **??**). The CTV target volume as well as the contours of the OAR were kept identical in both photon and carbon study, enabling a direct comparison of the treatment planning outcome.

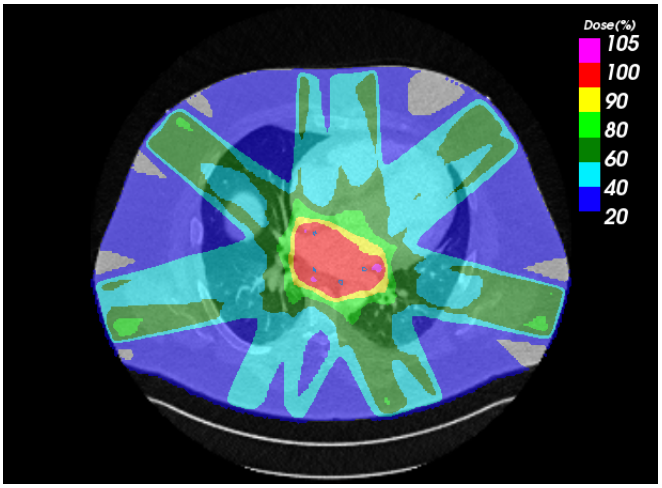

(a) Patient 2 : photons (IMRT)

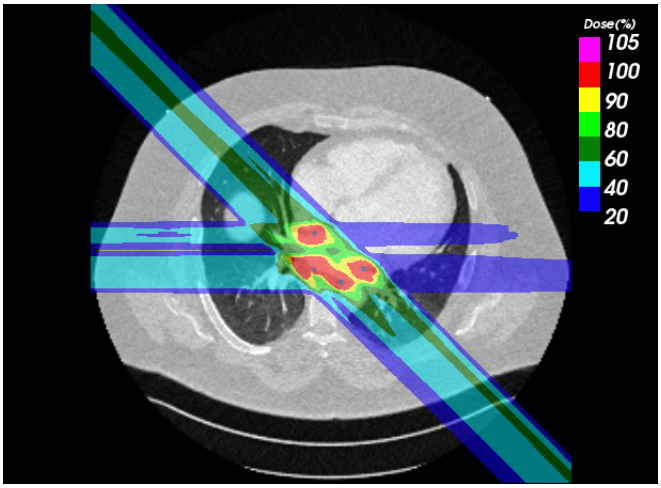

(b) Patient 2 : carbon ions (IMPT)

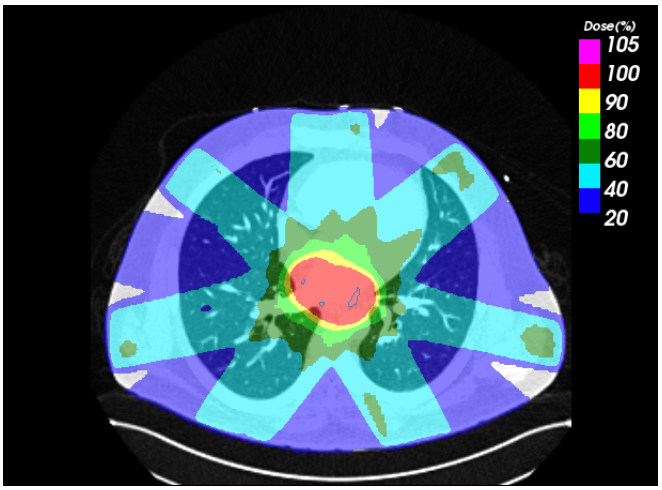

(c) Patient 4 : photons (IMRT)

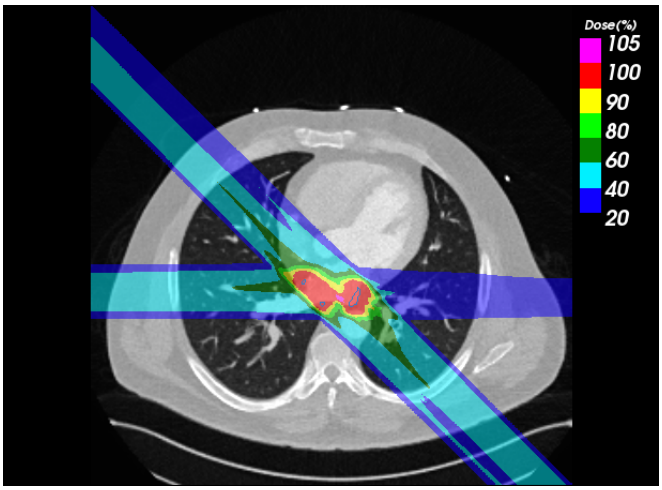

(d) Patient 4 : carbon ions (IMPT)

Figure 1.1: Comparison of dose cuts with photons (IMRT) and carbon ions (IMPT) treatment are shown for Patient 2 and Patient 4, respectively. As target volumes for the LPV and RPV the CTV is displayed. Photon treatment plans are courtesy of Dr. Amanda Deisher, Mayo Clinic, USA.

Table 1.1: Dose-volume limits for OARs. The volumes are stated in cc, dose values in Gy. The photon irradiation (IMRT) is compared with two different IMPT setting for carbon ions (weak: maximal 70% of the physical dose to the esophagus, strong: maximal 30%). The maximal applicable phyical dose to the target region for the dose-volume limits of the critical structures is stated in the last column for the strong IMPT setting.

Patient	OAR	Volume	Dose	endpoint	IMRT	IMPT (weak)	IMPT (strong)	max.D (strong IMPT)
2	Aorta / great vessels	10	31	Aneurysm	22.0	14.3	15.3	50.6
	Esophagus	5	11.9	Stenosis / fistula	24.6	22.5	7	42.5
	Heart	15	16	Pericarditis	27.1	25	25.3	(15.8)
	Trachea	4	10.5	Stenosis / fistula	7.6	4.3	3	87.5
4	Aorta / great vessels	10	31	Aneurysm	21.3	8.5	6.3	123.0
	Esophagus	5	11.9	Stenosis / fistula	20.2	18.5	3.5	85.0
	Heart	15	16	Pericarditis	26.1	20.5	16.8	(22.3)
	Trachea	4	10.5	Stenosis / fistula	0	0	0	∞

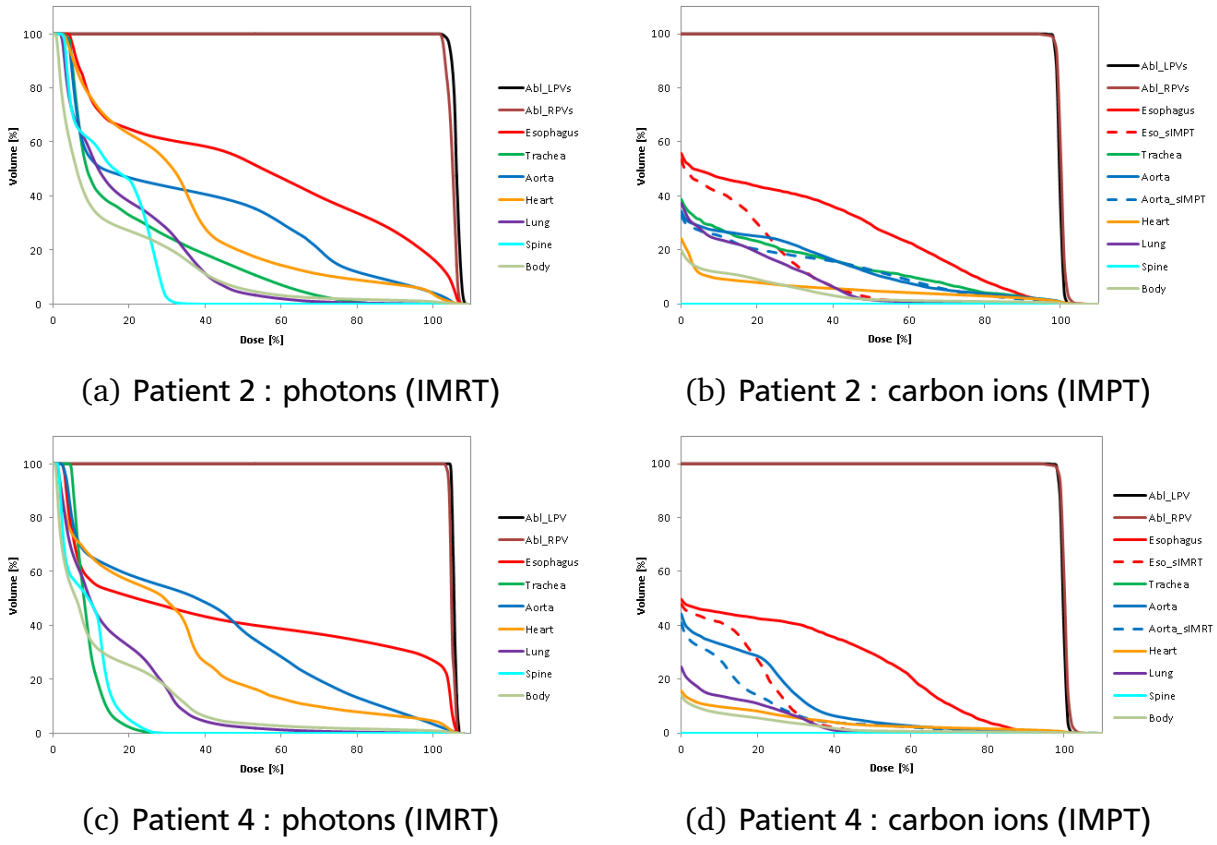

(a) Patient 2 : photons (IMRT)

(b) Patient 2 : carbon ions (IMPT)

(c) Patient 4 : photons (IMRT)

(d) Patient 4 : carbon ions (IMPT)

Figure 1.2: Comparison of DVHs are displayed for a treatment with photons (IMRT) versus carbon ions (IMPT). Target dose deposition are shown in black for the LPVs and brown for the RPVs, the dose to the esophagus is displayed in red, the trachea dose in green, the aorta dose in blue, the heart dose in orange, the lung dose in purple and the spinal cord dose in light blue. Photon treatment plans are courtesy of Dr. Amanda Deisher, Mayo Clinic, USA. For the carbon ion treatment plans different IMPT parameters are shown, where a better sparing of the esophagus is achieved with stronger limitation parameters, shown in dashed lines.

Table 1.2: Integral dose in [Gy×cm^3] for photon treatment (IMRT) and the two studied IMPT(OAR) deliveries for carbon ion irradiation (weak: maximal 70% of the physical dose to the esophagus, strong: maximal 30%).

Patient	OAR	IMRT	IMPT(OAR) (weak)	IMPT(OAR) (strong)
2	Esophagus	359	184	80
	Trachea	81	57	48
	Aorta	983	388	356
	Heart	13,863	2,340	2,123
	Lung	10,932	4,761	4,326
5	Esophagus	166	81	32
	Trachea	20	0	0
	Aorta	912	264	180
	Heart	6,992	1,029	874
	Lung	11,274	3,126	2,730

Due to the different interaction mechanism of photons and ions with matter (see chapter **??**, section **??**), and the resulting inverse depth dose profile of ions the surrounding tissue - including the OARs - can be better spared with carbon ions. Hence smaller field channel numbers can be chosen (see figure 1.1). The sparing of the OAR are shown both in the resulting dose-volume deposition to OARs in table 1.1 as well as in the comparison of the resulting DVHs for photons and carbon ions (see figure 1.2). For the carbon ion study two different IMPT parameter settings were used and both results are shown: An IMPT delivery with a weak dose restriction to the esophagus of maximal 70% of the physical dose of 25Gy and an IMPT setting with a stronger restriction of maximal 30% physical dose to the esophagus. As can be seen in table 1.1 the IMPT delivery with the weaker restriction results in dose-volume depositions comparable to the studied photon treatment, while the irradiation with the stronger dose restrictions to the esophagus results in a much better sparing of the studied OARs. An exception is the heart, as it is also the target volume itself. This structure requires a closer analysis on the irradiated substructures. Nevertheless it can already be seen from the DVH information of both patients, that the irradiated heart volume is drastically reduced with carbon ions compared to photons, due to the reduced number of beam channels feasible with carbon ions. The dose cut images (figure 1.1) also display that the left ventricles are better spared with a non-invasive irradiation of the PVs with carbon ions due to the chosen beam channel directions. It can thus be expected that this leads to a better sparing of the radiosensitive left coronary arteries.

Another method to compare the dose distribution for two different delivery techniques and quality beams is to calculate the integral dose, a measure of the total energy absorbed in the treated volume [Kha10]. It is calculated as the product of the mass of the irradiated tissue and the absorbed dose. Here, no organ specific density was assumed, but the integral dose was calculated as the dose volume product. The results for different critical structures (esophagus, trachea, heart, aorta and lung) are shown in table 1.2 and it can be seen that the absorbed energy of these organs can be drastically reduced with carbon ions compared to photons.

Porcine data

Photon treatment plans for the irradiation of the AV node were carried out on different CT phases for all four porcine data sets (see chapter **??**) as a five field IMRT treatment (see figure 1.3) with 6MV photons. In order to keep the ITV margin small the center phase of the motion was chosen as planning phase. This resulted in a treatment planning on 70% of the cardiac phase for Pig 1, on 20% for Pig 2, 0% (reference phase) for Pig 3 and 70% for Pig 4. The delivery was also planned as a single fraction irradiation of 25Gy. For the ITV additional 3mm isotropic expansions were used, resulting in the final PTV. For a fair comparison the shown carbon ion results were calculated on the same CT scan phases. The plans are SFUD irradiations with an isoptropic safety margin of 5mm to the CTV. The SFUD carbon ion plans were generated with two opposing beam channel directions (see chapter **??**). The target volume as well as the contours of the OAR were kept identical in both deliveries, enabling a direct comparison of the treatment planning outcome.

The sparing of the OARs are shown both in the resulting dose-volume deposition in table 1.3 as well as in the comparison of the resulting DVHs for photons and carbon ions (see figure 1.4). Due to the inverse depth-dose profile of carbon ions a reduced number of beam channel entry directions is feasible, resulting in a better sparing of the OARs compared to an irradiation of the AV node with photons. Due to the used beam channel directions it can be seen that the esophagus as well as the trachea do not receive any dose deposition. The dose deposition in the aorta is negligible, resulting in an irradiated volume of less than 10cc. Also the heart itself is much better spared with carbon ions, resulting in no dose-volume-limit exceeding irradiation for this structure. For photons on the other hand the limit is exceeded in three out of the four studied data sets. It should be noted that the analyzed heart volume excludes the irradiated AV node volume and hence the highest dose deposition, the target dose of 25Gy physical dose.

Also in the porcine data sets the body was only partially displayed on the CT scans and hence no density information could be derived for the calculation of the integral dose. The specific integral dose for both treatment delivery techniques were determined also for these cases. Thereby the sum over all dose volume products was calculated for the body contour volume. The results are shown in table 1.4 and it can be seen that the absorbed energy to the body volume can be drastically reduced with carbon ions compared to photons.

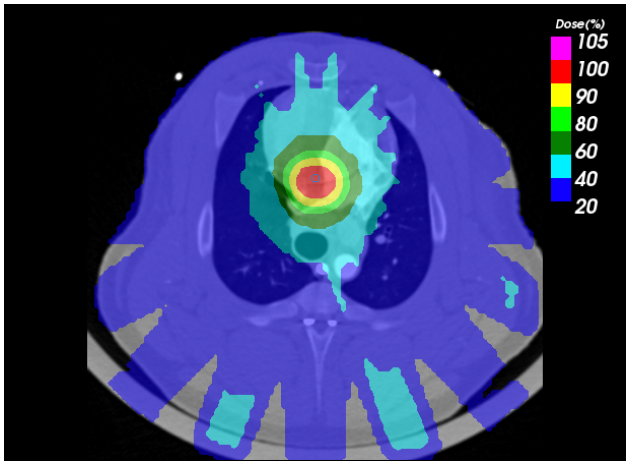

(a) Pig 3 : photons (IMRT)

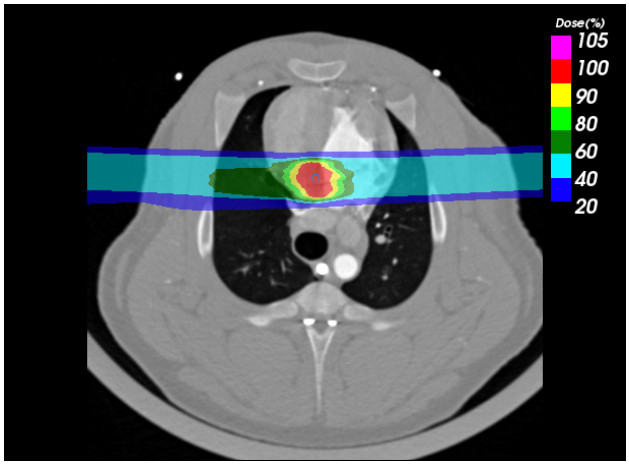

(b) Pig 3 : carbon ions (SFUD)

Figure 1.3: Comparison of dose cuts with photons and carbon ions treatment are shown for Pig 3. The photon delivery was planned as IMRT treatment and the carbon irradiation as SFUD irradiation, respectively. As the AV target volume the CTV is displayed. Photon treatment plans are courtesy of Dr.Limin Song, Mayo Clinic, USA.

Table 1.3: Dose-volume limits for OARs. The volumes are stated in cc, dose values in Gy. The photon irradiation (IMRT) is compared with SFUD carbon ion irradiation

Pig	OAR	Volume	Dose	endpoint	IMRT	SFUD
1	Aorta / great vessels	10	31	Aneurysm	1.1	0.0
	Esophagus	5	11.9	Stenosis / fistula	0.2	0.0
	Heart	15	16	Pericarditis	18	6.3
	Trachea	4	10.5	Stenosis / fistula	6.5	0.0
2	Aorta / great vessels	10	31	Aneurysm	2.1	0.0
	Esophagus	5	11.9	Stenosis / fistula	0.4	0.0
	Heart	15	16	Pericarditis	16.1	6.5
	Trachea	4	10.5	Stenosis / fistula	2.6	0.0
3	Aorta / great vessels	10	31	Aneurysm	0.9	0.0
	Esophagus	5	11.9	Stenosis / fistula	0.3	0.0
	Heart	15	16	Pericarditis	23	4.8
	Trachea	4	10.5	Stenosis / fistula	0.2	0.0
4	Aorta / great vessels	10	31	Aneurysm	0.7	0.0
	Esophagus	5	11.9	Stenosis / fistula	0.3	0.0
	Heart	15	16	Pericarditis	14.3	7.3
	Trachea	4	10.5	Stenosis / fistula	4.6	0.0

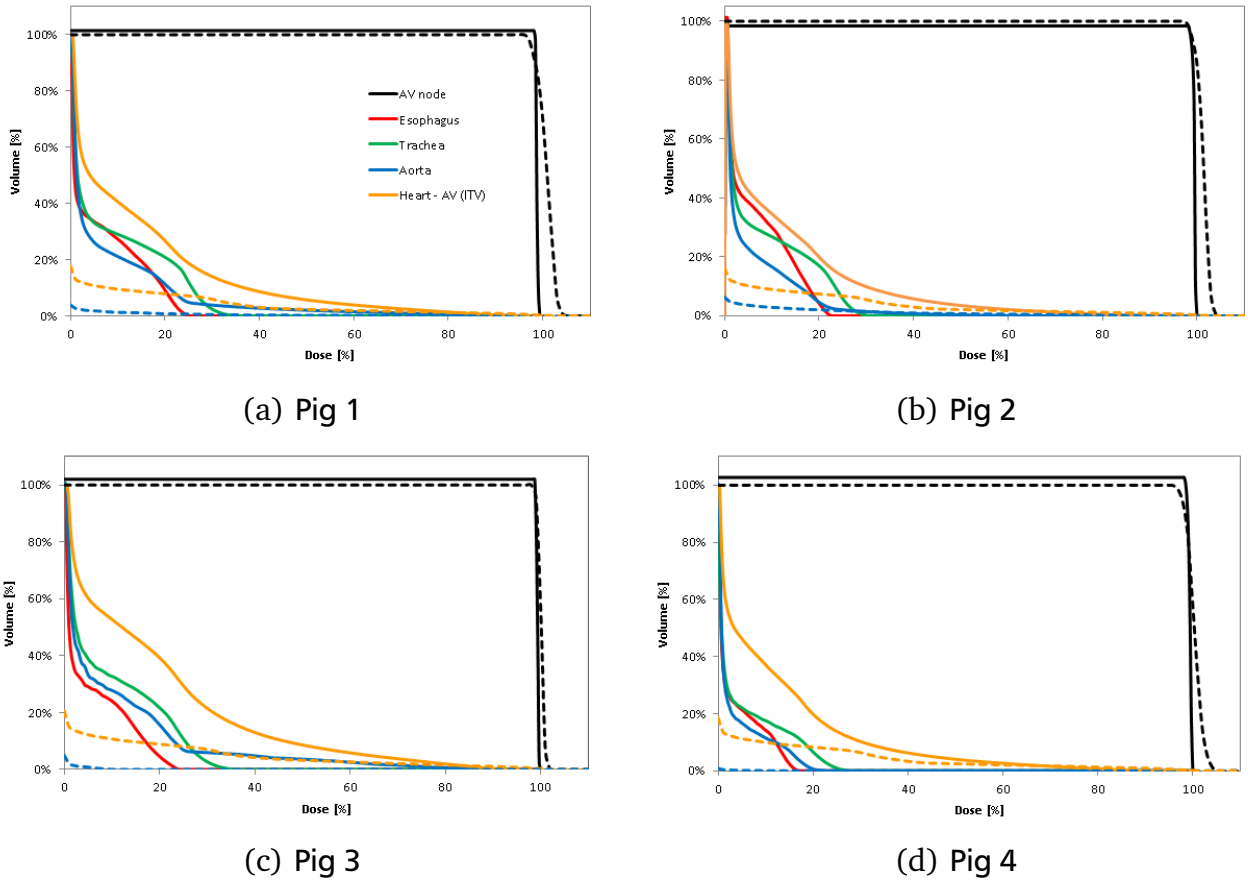

(a) Pig 1 (b) Pig 2

(c) Pig 3 (d) Pig 4

Figure 1.4: Comparison of DVH results with photons (solid) and carbon ions (dashed). The photon delivery was planned as IMRT treatment and the carbon irradiation as SFUD irradiation, respectively. The target dose to the AV node is displayed in black, the dose to the esophagus in red, to the trachea in green, the aorta in blue and the irradiated heart (with the substracted the ITV bolume of the AV node) is shown in orange. In case of carbon SFUD deliveries, the esophagus and trachea do not receive any dose. Photon treatment plans are courtesy of Dr. Limin Song, Mayo Clinic, USA.

Table 1.4: Integral dose in [Gy×cm^3], exemplarily for pig 3, for photon irradiation (IMRT) and carbon ion treatment (SFUD).

Pig	OAR	IMRT	SFUD
3	Esophagus	14	0
	Trachea	62	0
	Aorta	66	1
	Heart	1,374	289
	Lung	1,195	187

1.2 Treatment planning of cardiac target volumes with scanned ions

In order to assess the displacement of the cardiac volumes due to respiration and heartbeat, 4DCTs gated on respiration or heartbeat were analyzed and the findings will be discussed in section 1.2.1. Afterwards the usage of contrast enhanced CT scans due to the poor contrast between the heart muscle and the contained blood will be discussed in section 1.2.2 and possible experimental solutions for resulting range uncertainties will be proposed. In section 1.2.3 the result of the used motion mitigation techniques for the irradition of cardiac target volumes with a scanned carbon ion beam will be deliberated.

1.2.1 Motion of cardiac volumes

Target volumes in the heart move on one hand due to the respiration of the patient, a motion with a large amplitude and a slow cycle time of ten to fifteen respiratory cycles per minute, and on the other hand due to heartbeat, a motion with a small amplitude and cycle time of sixty to eighty beats per minutes. Even though both motions occur simultaneously in patients, they were studied independently in the here presented treatment planning studies. This can be justified as a CT gated to both motion types would require long CT acquisitions and hence unnecessary dose exposures to the patient.

PVs motion in humans

The motion of PVs ablation sites in humans due to respiration were studied based on respiratory gated time resolved computed tomographies (4DCTs) of nine lung cancer patients, recorded for radiotherapy at MD Anderson Cancer Center (MDACC), USA. The heartbeat influence was studied on cardiac gated 4DCTs of five AF patients, recorded at Mayo Clinic, USA.

The movement of the ablation sites of the PVs were studied in the three motion directions (superior-inferior (SI), anterior-posterior (AP) and left-right (LR)) as well as for the absolute displacement. Different studies concerning the PVs displacement due to respiration can also be found in literature [Ect08] [Nos05], as breathing is also relevant for cather ablation due to the reduction in catheter tip contact force [Kum12]. While Ector et al. stated an absolute mean displacement of (19.1 $\pm$ 8.6)mm for both LPV and RPV, a much smaller absolute mean displacement of (6.76 $\pm$ 3.57)mm and (6.76 $\pm$ 2.51) was found in the here studied patient cohort for LPV and RPV, respectively. The SI motion was the biggest motion direction with a mean displacement of (-6.41 $\pm$ 3.80)mm for LPV and (-6.57 $\pm$ 2.42)mm for RPV. AP and LR directions were almost negligible with a mean motion of less than 2mm. The difference between the two cardiac sites is more pronounced in AP and LR, so that e.g. the LPV move more

in anterior direction. In LR direction a difference between LPV and RPV motion resulted, where the mean displacement of the LPV is almost double compared to the RPV. Ector et al. on the other hand found a mean displacement of (14.6 ± 7.7)mm in inferior direction, (9.7 ± 7.6)mm in anterior direction and (0.4 ± 3.8)mm in the left direction, hence concluding a much bigger displacement in SI and AP directions. It remains to be analyzed if this discrepancy is due to the here studied lung tumor patient cohort in comparison to the AF patients studied by Ector et al.. Nevertheless it should be noted that both analysis are based on a small patient number of nine patients compared to sixteen patients.

The motion of the ablation sites for the PVs due to heartbeat was studied for the left and right structures, respectively, in the three above stated motion directions. Only a small mean absolute displacement over all patients of less than 3mm was observed. The biggest absolute displacement reached a mean value of up to (6.5 ± 3.0)mm in one patient case for the RPV and (5.5 ± 3.1)mm for the LPV. No dominant motion direction was found, even though a tendency to a bigger motion in AP direction could be assumed. Furthermore, no motion pattern could be derived from the five studied patient data sets, indicating that the underlying motion causing the PV ablation sites to move is much more complex and the result of different motion influences. For further studies concerning the PV displacement due to heartbeat, the reader should be refered to Lickfett et al. [Lic05] and Patel et al. [Pat08]. Lickfett et al. found comparable maximal displacements of up to 7.2mm in some of the healthy volunteers. Patel et al., who studied the displacement in thirty AF patients, stated mean values in the order of 3mm. The here presented results are hence in good agreement with the literature values.

Motion in porcine due to heartbeat

The motion of different potential cardiac ablation sites (AV node, CTI and PVs) were studied in pigs based on cardiac gated 4DCTs of four swines, recorded at Mayo Clinic, USA. The acquired CT scans were both native and contrast enhanced. It was found that native CT scans do not enable an assessment of the cardiac target volume displacement due the low contrast between the cardiac muscle and the contained blood. Analysis was hence carried out on the contrast enhanced CT scans. Concerning the motion of the three studied potential target sites it could be stated that the PVs moved to the smallest extent (maximal displacement of up to 5mm), followed by the AV node (maximal displacement of up to 6mm) and that the CTI moved the most (maximal displacement of 7mm). It was speculated that this is due to the location of the volumes, where a proximal location on or near the ventricles lead to a larger movement. Even though also in the porcine data sets no maximal motion phase or motion pattern could be observed due to heartbeat it was found that the displacement was shallower between certain motion phases (motion phase 6 to 13) and hence, contrary to the studied human data, gating

could be an optional motion mitigation technique. Moreover, in comparison to the human data, the displacement in AP direction in the porcine data was clearly larger than in the other two studied directions.

1.2.2 Contrast enhanced CT scans

Particle treatment planning needs to be carried out on native CT scans in order to obtain the correct range information [Wer04]. In case of the intended irradiation of cardiac target volumes it was found that native CT scans do not provide sufficient contrast between the heart muscle and the contained blood. As stated, the motion information can thus only be assessed from contrast-enhanced CT scans. It needs to be studied if the displacement vector field obtained from registration on the contrast enhanced CT scans yield a good enough agreement when directly used on the native data sets for the actual treatment planning. The resulting range uncertainties need to be carefully considered, especially regarding the dose to critical structures like the esophagus. Analog to studies by e.g. el Bentefour et al. [Ben12], where in vivo range verifications were successfully achieved with a small dose deposition (<0.5cGy) in silicone diodes, a possible solution could be to predeposit the resulting treatment plan with a small dose in the order of mGy. By placing such an detector with a catheter inside the patient, either in front of or inside the esophagus, it would allow to test for range of the planned energies and hence for potential miscalculation or interfractional changes of the organs. Range uncertainties to the target area could furthermore be corrected before irradiation with the total single fraction dose. By using in-beam PET monitoring with ^{11}C and ^{10}C fragments (see chapter **??**, section **??**) it would be possible to irradiate a low dose in order to detect the range and position uncertainties. This was already carried out at GSI, where ^{10}C resulted to be best suited as a probing beam for range verifications [Lin12]. The accuracy of PET monitoring for ion range determination was studied by Fiedler et al. [Fie10] for more than 80 of the 400 patients irradiated in the GSI pilot project. It was stated that in-beam PET method demonstrated a high sensitivity for the detection of range deviations and would thus be beneficial for the here presented treatment modality.

1.2.3 Motion mitigation techniques

Due to the large motion of the PV ablation sites induced by the respiratory motion in the studied patient cohort, interplay was oberved to lead to strong underdosage, so that in some cases only V95=70% was achieved with no safety margin and V95=80% with safety margins of 5mm. Due to the large motion amplitude of more than 1cm gating was studied as potential motion mitigation technique (see section 1.2.3). For the displacements induced by heartbeat a smaller motion of less than 1cm was observed in all studied human data, so that rescanning was studied as an adequate motion mitigation technique for this case. As expected, the interplay effect in this case was smaller than for respiration, with minimal underdosages of V95=85% for no safety margin and a minimal V95 of 92% for 5mm and 7mm margin, respectively. Even though this underdosage with safety margin already yields a clinically acceptable dose coverage the usage

of an additional motion mitigation technique leads to a more robust treatment delivery, as is stated in 1.2.3. For the porcine data, where the motion influence of the heartbeat on the AV node target volume was studied and only a single margin of 5mm was used, the interplay effect led to larger minimal underdosages of 56% in some of the studied pig data sets. Hence the usage of rescanning as motion mitigation technique was also needed in this case.

Respiratory motion

In the animal model studies by Sharma et al. [Sha10] the target displacement due to respiration was tracked with the CyberKnife system. In the study by Blanck et al. [Bla13] an ITV approach was used for the respiratory motion. Here, gating was used as a potential motion mitigation technique. It is suited for larger target displacments, since only a fraction of the motion cycle is used. The gating window is positioned at end exhale, enabling a more robust delivery with only a small amount of residual motion. To this date, gating is already used in ion beam centers with passive particle delivery [Min00] as well as in IMRT treatments in photon centers [Kea06]. A pilot study with scanned carbon ions was recently conducted on liver patients at HIT by using gating and abdominal compression [Ric12]. In the here studied case, gating was found to be an adequate motion mitigation technique so that underdosages could be increased up to a minimum of 98% for all studied safety margins and patient cases. Even in cases with no safety margin underdosage could be increased to a minimum of 94%. It can nevertheless be stated that safety margins, which are needed in order to account for e.g. position inaccuracies, improved the outcome and made the delivery more robust. It was furthermore studied in two patient data sets if the treatment outcome improved when rescanning was applied for the residual motion inside the gating window. This is proposed as phase-controlled rescanning [Fur07] or breath-sampled rescanning [Sec09]. It resulted in a marginal improvement compared to only gating, whereas no improvement was observed when using more than ten rescans. Since the irradiation of the PV ablation sites were also studied to include rescanning as mitigation for heartbeat motion, the combination of these two techniques will be naturally achieved. Concerning the treatment time it was expected that gating would increase the treatment time dependence on the used gating window. Since only 30% of the motion cycle was used for irradiation, the treatment resulted into a delivery time of about 30min with a high intensity of 55,000 minimum particles per beam spot and for a safety margin of 3mm. Compared to the radiofrequency ablation procedure which takes up to a couple of hours, and to the photon irradiation of up to two hours [Sha10], the treatment time is drastically reduced. This was found for the HIT beam parameters, where a relatively long time for an energy change is needed. The particle intensity could be further increased, leading to an even further reduced treatment time. Nevertheless it was shown that very high intensities can endanger a homogenous dose coverage [Mue14]. New accelerator concepts with variable excitation cycles [Tsu08] or faster energy changes [Iwa10]

might hence be needed. An alternative to gating could be the usage of apneic oxygenation, which is currently used at the Rinecker Proton Therapy Center in Munich [Ber11] [RPTC12] for the treatment of tumors in the upper abdomen and thorax. This approach will also be used in the planned animal experiments with pigs which will be carried out at GSI in the summer of 2014.

Heartbeat motion

In the animal model studies by Sharma et al. [Sha10] and by Blanck et al. [Bla13] an ITV approach was used for the heartbeat motion. In the here presented study rescanning was used as a motion mitigation technique for heartbeat motion, both in human as well as for the porcine data sets. Especially in human data only rescanning seemed to be an adequate technique due to the lack of a motion pattern or a region of shallower motion. For the porcine data on the contrary, cardiac gating might be another option, which needs to be investigated. In the human data it was found that the dose coverage was higher than 99% in about 96% of the studied cases with safety margins over 3mm. This result could be even further improved if ten or more rescans were applied. Nevertheless it can be argued that five rescans already yield a very good dose deposition in the target volume. For the porcine data and the studied AV node ablation it was found that the dose coverage was higher than 99% in 85% of the studied cases with a safety margin of 5mm. This finding could be slightly improved to 91% of the studied cases for ten rescans. A higher rescan number of fifteen rescans did not lead to a significant improvement. The finding indicates that ten rescans are already sufficient to enable a robust and stable irradiation of the cardiac target volume in the presence of heartbeat. Due to the high single dose the resulting intensity per rescan is expected to be large and hence the application should be feasible without further prolonging the treatment time. All the studied rescanning results were obtained for slice-by-slice rescanning. This means that each IES is rescanned independently with the predefined numbers of rescans. In other studies it has nevertheless be found that other rescan methods, like e.g. breath-sampled rescanning [Sec09] or phase-controlled rescanning [Fur07], result in an increased robustness while requiring fewer rescan numbers compared to slice-by-slice rescanning as it breaks up possible synchronicities between beam application and target motion [Mue14]. In breath-sampled rescanning the IES are rescanned individually, but the rescans are sampled according the motion phase of the breathing period, so that every motion phase receives dose appliactions. An analog delivery according to the heartbeat and hence an ECG-sampled rescanning might be feasible and could lead to improved results.

Bibliography

[Ami06] Amino M, Yoshioka K, Tanabe T, Tanaka E, Mori H, Furusawa Y, Zareba W, Yamazaki M, Nakagawa H, Honjo H, Yasui K, Kamiya K, Kodama I: Heavy ion radiation up-regulates Cx43 and ameliorates arrhythmogenic substrates in hearts after myocardial infarction; Cardiovascular Research; 72; 412?421; 2006

[Ami10] Amino M, Yoshioka K, Fujibayashi D, Hashida T, Furusawa Y, Zareba W, Ikari Y, Tanaka E, Mori H, Inokuchi S, Kodama I, Tanabe T: Year-long upregulation of connexin43 in rabbit hearts by heavy ion irradiation; Am J Physiol Heart Circ Physiol; 298; 2010.

[Ben12] Bentefour el H, Shikui T, Prieels D, Lu HM: Effect of tissue heterogeneity on an in vivo range verification technique for proton therapy; Phys Med Biol.; 57(17):5473-84; 2012

[Bik11] Bikou O, Thomas D, Trappe K, Lugenbiel P, Kelemen K, Koch M, Soucek R, Voss F, Becker R, Katus HA, Bauer A:Connexin 43 gene therapy prevents persistent atrial fibrillation in a porcine model; Cardiovasc Res.; 92(2); 2011

[Bis65] Bishop VS, Stone HL, Yates J, Simek J, Davis JA: Effects of external irradiation of the heart on cardiac output, venous pressure and arterial pressure; J Nucl Med.; 1965

[Chr13] Christodouleas JP, Tang S, Susil RC, McNutt TR, Song DY, Bekelman J, Deville C, Vapiwala N, Deweese TL, Lu HM, Both S: The effect of anterior proton beams in the setting of a prostate-rectum spacer; Med Dosim.;38(3); 2013

[Efs56] Efskind D: The Effect of Massive X-ray Doses to the Mediastinum, Especially the Heart. Oslo, Norsk Hydro's Institute for Cancer Research Report 1954-1956, 1956, pp. 13-14

[Faj70] Fajardo LF and Stewart JR: Capillary Injury Preceding Radiation-Induced Myocardial Fibrosis; Radiology; 101; 1971

[Faj73] Fajardo, LF and Stewart JR: Pathogenesis of radiation-induced myocardial fibrosis; Laboratory Investigations; 29; 1973

[Fie10] Fiedler F, Shakirin G, Skowron J, Braess H, Crespo P, Kunath D, Pawelke J, Pnisch F, Enghardt W: On the effectiveness of ion range determination from in-beam PET data; Phys Med Biol; 55(7); 2010

[Gys14] van Gysen K, Kneebone A, Alfieri F, Guo L, Eade T: Feasibility of and rectal dosimetry improvement with the use of SpaceOAR® hydrogel for dose-escalated prostate cancer radiotherapy; J Med Imaging Radiat Oncol; 2014

[Kan04] Kanagaratnam P, Cherian A, Stanbridge RD, Glenville B, Severs NJ, Peters NS: Relationship between connexins and atrial activation during human atrial fibrillation; J Cardiovasc Electrophysiol; 15; 206?216; 2004

[Kea06] Keall PJ1, Mageras GS, Balter JM, Emery RS, Forster KM, Jiang SB, Kapatoes JM, Low DA, Murphy MJ, Murray BR, Ramsey CR, Van Herk MB, Vedam SS, Wong JW, Yorke E: The management of respiratory motion in radiation oncology report of AAPM Task Group 76; Med Phys.; 33(10); 2006

[Kha10] Faiz M. Khan: The physics of radiation therapy; 4th edition; Lippincott Williams & Wilkins; 2010

[Lin12] Linz U: Ion Beam Therapy - Fundamentals, Technology and Clinical Applications; Springer; chapter 31: Online Irradiation Control by Mean of PET by Fiedler F, Kunath D, Priegnitz M and Enghardt W; p.535; 2012

[Phi64] Phillips SJ, Reid JA and Rugh R: Electrocardiographic and patholic changes after cardiac X-irradiation in dogs; American Heart Journal; 68; 1964

[Pol01] Polontchouk L, Haefliger J-A, Ebelt B, Schafer T, Stuhlmann D, Mehlhorn U et al: Effects of chronic atrial fibrillation on gap junction distribution in human and rat atria; J Am Coll Cardiol; 38; 883?891; 2001

[Ruc13] Ruciński A, Bauer J, Campbell P, Brons S, Unholtz D, Habl G, Herfarth K, Debus J, Bert C, Parodi K, Jäkel O, Haberer T: Preclinical investigations towards the first spacer gel application in prostate cancer treatment during particle therapy at HIT; Radiat Oncol.; 8:134; 2013

[Sev04] Severs NJ, Coppen SR, Dupont E, Yeh H-I, Ko Y-S, Matsushita T: Gap junction alterations in human cardiac disease; Cardiovascular Research; 62; 368?377; 2004

[Sev08] Severs NJ, Bruce AF, Dupont E and Rothery S: Remodelling of gap junctions and connexin expression in diseased myocardium; Cardiovascular Research; 80; 9?19; 2008

[Ste68] Stewart JR, Fajardo LF, Cohn K and Page V: Experimental Radiation-Induced Heart Disease in Rabbits; Radiology 91; 1968

[Vis13] Viswanathan AN, Damato AL, Nguyen PL: Novel use of a hydrogel spacer permits reirradiation in otherwise incurable recurrent gynecologic cancers; J Clin Oncol.; 31(34); 2013

[Wer04] Wertz H and Jäkel O: Influence of iodine contrast agent on the range of ion beams for radiotherapy; Med Phys.; 31(4); 767-73; 2004

[Yeh01] Yeh H-I, Lai Y-J, Lee S-H, Lee Y-N, Ko Y-S, Chen S-A et al: Heterogeneity of myocardial sleeve morphology and gap junctions in canine superiorvena cava; Circulation; 104; 3152?3157; 2001

[Fur07] Furukawa T, Inaniwa T, Sato S, Tomitani T, Minohara S, Noda K, Kanai T: Design study of a raster scanning system for moving target irradiation in heavy-ion radiotherapy; Med Phys.; 34(3); 2007

[Ber11] Bert C and Durante M: Motion in radiotherapy: particle therapy; Phys Med Biol.; 56(16); 2011

[Sec09] Seco J, Robertson D, Trofimov A, Paganetti H: Breathing interplay effects during proton beam scanning: simulation and statistical analysis; Phys Med Biol.; 54(14); 2009

[Mue14] Muessig D: Re-scanning in scanned ion beam therapy in the presence of organ motion; Dissertation; TU Darmstadt; 2014

[RTOG0631] RTOG 0631 Protocol Information: Phase II/III Study of Image-Guided Radiosurgery/SBRT for Localized Spine Metastasis; 2011

[RTOG0915] RTOG 0915 Protocol Information: A Randomized Phase II Study Comparing 2 Stereotactic Body Radiation Therapy (SBRT) Schedules for Medically Inoperable Patients with Stage I Peripheral Non-Small Cell Lung Cancer; 2010

[Sha10] Sharma A, Wong D, Weidlich G, Fogarty T, Jack A, Sumanaweera T, Maguire P: Noninvasive stereotactic radiosurgery (CyberHeart) for creation of ablation lesions in the atrium; Heart Rhythm 7(6); 802-810; 2010

[Gag10] Gagliardi G, Constine LS, Moiseenko V, Correa C, Pierce LJ, Allen AM, Marks LB: Radiation dose-volume effects in the heart; Int J Radiat Oncol Biol Phys.;7 6(3 Suppl); 2010

[Carm76] Carmel RJ, Kaplan HS: Mantle irradiation in Hodgkin's disease. An analysis of technique, tumor eradication, and complications; Cancer; 37(6); 1976

[Wei08] Wei X, Liu HH, Tucker SL, Wang S, Mohan R, Cox JD, Komaki R, Liao Z: Risk factors for pericardial effusion in inoperable esophageal cancer patients treated with definitive chemoradiation therapy; Int J Radiat Oncol Biol Phys.; 70(3); 2008

[Han93] Hancock SL, Tucker MA, Hoppe RT; Factors affecting late mortality from heart disease after treatment of Hodgkin's disease; JAMA; 270(16); 1993

[Tay07] Taylor CW, Nisbet A, McGale P, Darby SC: Cardiac exposures in breast cancer radiotherapy: 1950s-1990s; Int J Radiat Oncol Biol Phys.; 69(5); 2007

[Hoo07] Hooning MJ, Botma A, Aleman BM, Baaijens MH, Bartelink H, Klijn JG, Taylor CW, van Leeuwen FE: Long-term risk of cardiovascular disease in 10-year survivors of breast cancer; J Natl Cancer Inst.; 99(5); 2007

[Dar13] Darby SC, Ewertz M, McGale P, Bennet AM, Blom-Goldman U, Brnnum D, Correa C, Cutter D, Gagliardi G, Gigante B, Jensen MB, Nisbet A, Peto R, Rahimi K, Taylor C, Hall P: Risk of ischemic heart disease in women after radiotherapy for breast cancer; N Engl J Med.; 368(11); 2013

[Mar98] Martel MK, Sahijdak WM, Ten Haken RK, Kessler ML, Turrisi AT: Fraction size and dose parameters related to the incidence of pericardial effusions; Int J Radiat Oncol Biol Phys.; 40(1); 1998

[Ect08] Ector J, De Buck S, Loeckx D, Coudyzer W, Maes F, Dymarkowski S, Bogaert J, Heidbüchel H: Changes in left atrial anatomy due to respiration: impact on three-dimensional image integration during atrial fibrillation ablation; J Cardiovasc Electrophysiol; 19(8); 828-34; 2008

[Nos05] Noseworthy PA, Malchano ZJ, Ahmed J, Holmvang G, Ruskin JN, and Reddy VY: The impact of respiration on left atrial and pulmonary venous anatomy: Implications for image-guided intervention; Heart Rhythm; 2; 1173?1178; 2005

[Kum12] Kumar S, Morton JB, Halloran K, Spence SJ, Wong MCG, Kistler PM, Kalman JM: Effect of respiration on catheter-tissue contact force during ablation of atrial arrhythmias; Heart Rhythm; Vol 9; No 7; 2012

[Lic05] Lickfett L, Dickfeld T, Kato R, Tandri H, Vasamreddy CR, Berger R, Bluemke D, Lderitz B, Halperin H, Calkins H: Changes of pulmonary vein orifice size and location throughout the cardiac cycle: dynamic analysis using magnetic resonance cine imaging; J Cardiovasc Electrophysiol.; 16(6); 2005

[Pat08] Patel AR, Fatemi O, Norton PT, West JJ, Helms AS, Kramer CM, Ferguson JD: Cardiac cycle-dependent left atrial dynamics: implications for catheter ablation of atrial fibrillation; Heart Rhythm; 5(6); 2008

[Bla13] Blanck O, Bode F, Gebhard M, Hunold P, Brandt S, Bruder R, Schweikard A, Grossherr M, Rades D and Dunst J: Radiochirurgisch erzeugte Läsionen im Antrum der Pulmonarvenen: Vorläufige Ergebnisse im Tiermodell und mögliche Implikationen für die Behandlung von Vorhofflimmern; DEGRO 2013

[Min00] Minohara S, Kanai T, Endo M, Noda K and Kanazawa M: Respiratory gated irradiation system for heavy-ion radiotherapy; Int. J. Radiat. Oncol. Biol. Phys.; 47(4); 1097-1103; 2000

[Ric12] Richter D: Treatment planning for tumors with residual motion in scanned ion beam therapy; Dissertation; TU Darmstadt; 2012

[RPTC12] Erfahrungsbericht zweiter Monat klinischer Betrieb RPTC; Mai 2009; Internet Communication

[Mue14] Muessig D: Re-scanning in scanned ion beam therapy in the presence of organ motion; Dissertation; TU Darmstadt; 2014

[Iwa10] Iwata Y,Kadowaki T, Uchiyama H, Fujimoto T, Takada E, Shirai T, Furukawa T, Mizushima K, Takeshita E, Katagiri K, Sato S, Sano Y, Noda K: Multiple-energy operation with extended flattops at HIMAC; Nuclear Instruments and Methods in Physics Research Section A; 624, 2010

[Tsu08] Tsunashima Y, Vedam S, Dong L, Umezawa M, Sakae T, Bues M, Balter P, Smith A, Mohan R: Efficiency of respiratory-gated delivery of synchrotron-based pulsed proton irradiation; Phys Med Biol.; 53(7); 2008